

# ON THE POSSIBILITY OF REUSING ELECTRON RINGS FOR HEAVY-ION ACCELERATION

YU. I. ALEXAHIN and V. P. SARANTSEV

*Department of New Acceleration Methods,  
Joint Institute for Nuclear Research, Dubna, USSR*

*(Received April 10, 1984)*

A concept of a shuttle electron ring accelerator (SHERA) for heavy ions is considered. Each electron ring is used for magnetostatic acceleration of ions many times, thus increasing the output ion current. The following problems are treated: the optimal static magnetic-field configuration; the requirements on the pulsed system that restores the electron ring to the initial state; the coherent stability of the ring; limitations on the electron ring life-time connected, in particular, with emittance growth during separation of ions. It is shown that with electron rings of presently achieved quality, SHERA can yield a uranium beam with energy 10 MeV/nucleon and intensity  $3 \times 10^{13}$  ions/sec.

## I. INTRODUCTION

An intense beam of accelerated heavy ions can find a variety of applications both in research (synthesis of superheavy elements, study of shock waves in nuclei, search for new nuclear phase states) and in applied physics (inertial confinement fusion, production of microfilters, ion implantation, etc.) as well.

Collective acceleration by electron rings, proposed by V. I. Veksler *et al.*,<sup>1</sup> still remains one of the most promising methods of heavy-ion acceleration. The feasibility of the method has been demonstrated in experiments on the JINR Collective Heavy Ion Accelerator prototype.<sup>2</sup> The acceleration of ions with atomic mass  $A = 12$  to 16 by rings with electron number  $N_e \approx 10^{13}$  has been observed; the energy gain per nucleon was found to be  $10Z/A$  MeV/m, where  $Z$  is the average charge of ions. Electron rings with similar parameters were formed in a series of "Compressor" devices at Berkeley.<sup>3</sup>

The ion-beam intensity is proportional to the accelerator repetition rate, which is hard to have exceed 50 to 100 pps due to high power dissipation in the electron-beam injector (induction linac) and in the compressor.

The output ion current can be significantly increased by multiple use of each electron ring. In the case of light ions, such mode of acceleration, which may be called a "shuttle mode", was considered in Ref. 4. Acceleration of heavy ions by electron rings has some new features arising from the necessity to trap the ring for reloading with ions and from significant electron energy transfer to the accelerated ions. The corresponding modification was proposed and studied in Ref. 5. The analysis has revealed the principal difficulties in realization of the scheme. The main obstacle found is heating of the electrons during the non-adiabatic process of interception of the returning ring.

In the present paper, we consider a concept of shuttle electron ring accelerator (SHERA) of heavy ions that allows one to avoid these difficulties.

## II. GENERAL SCHEME OF SHERA

Let us review briefly the concept of shuttle acceleration proposed in Ref. 4, 5. The electron ring formed in a compressor is loaded with ions and accelerated by expansion into a decreasing static magnetic field  $B_z(Z)$ . The field gradient satisfies the condition of holding the ions<sup>2</sup>

$$B_r \approx -\frac{r_0}{2} \cdot \frac{\partial B_z}{\partial Z} \leq k \frac{\xi + 1}{\xi} f \frac{2|e|N_e}{\pi\beta_\theta r_0(a_r + a_z)} \quad (1)$$

where  $r_0$  is the ring major radius,  $a_{r,z}$  are the ring cross-section half-dimensions,  $f = ZN_i/N_e$  is the charge neutralization factor,  $\xi = m_n AN_i/m_e \gamma N_e$  is the loading factor,  $\beta_\theta$  and  $\gamma$  denote the electrons' azimuthal velocity (in units of the speed of light  $c$ ) and relativistic mass factor,  $m_{e,n}$  are the rest masses of an electron and a nucleon,  $k = 0.25 \div 0.33$  is the safety factor and  $N_i$  is the number of ions in the ring.

Having passed the acceleration section, the electron-ion ring enters the region of steeply rising magnetic field (magnetic mirror) where the holding condition<sup>1</sup> is not satisfied. The ions are shaken out of the electron ring, which reflects from the mirror and returns to the starting position to be reloaded with ions. The electron energy partially transferred to the ions is replenished by periodic passing through a cavity<sup>4</sup> or by inductive electric field in a "manipulator"<sup>5</sup> that traps the electron ring for reloading.

Besides the difficulties of ring interception by the manipulator, there are some other reasons to consider the scheme unfit for acceleration of heavy ions. In order to return to the region of strong magnetic field, the electrons can give only a small fraction of their energy to ions, which limits  $N_i$  by values of order  $10^{11}$  A. Then to compete with a single-shot scheme, the ring cycling frequency has to be very high ( $\sim 100$  kHz), which interferes with reaching high ion charge states and hence makes it necessary to increase drastically the length of the accelerator.

The situation becomes more favorable if the restriction on amount of energy transferred is removed and larger loading factor values ( $\xi \gg 1$ ) are admitted. Then the increase in number of ions in a ring compensates for the decrease in cycling frequency. Having imparted a significant portion of its rotational energy to ions, the electron ring will oscillate at the bottom of the magnetic potential well with small amplitude (compared with the length of acceleration). It can be returned to the start positioning using an artificial slow-wave line in analogy with rapid-cycle compressor<sup>6</sup> operation. The inductive electric field generated by propagating over the line current pulse fully restores the electron energy spent on acceleration of ions, as can easily be seen from the generalized momentum-conservation law. As the velocity of the wave in the line is low ( $v_\phi/c \lesssim 10^{-3}$ ) it does not give a problem in intercepting the ring in the starting region adiabatically.

The corresponding scheme of SHERA is shown in Fig. 1. The electron ring formed in compressor 1 (of dynamic or static type) is loaded with ions and retained in "waiting-room" 2 for the time needed to reach the desired ion charge state. Then oppositely-connected starting coils 3 are switched on, removing the magnetic potential barrier and pushing the electron-ion ring out into the decreasing magnetic field formed by (superconducting) solenoid 4. Inside the solenoid, there are coils 5 and capacitors 6 of an artificial line which returns the electron ring to the initial state after the ions are separated from it in the field of the reflecting coils 7. Axially slit screens 8, so called "squirrel cages",<sup>7</sup> provide the electron ring focusing after the separation and reduce the binding energy of the ring components. The electron ring can be reloaded with ions

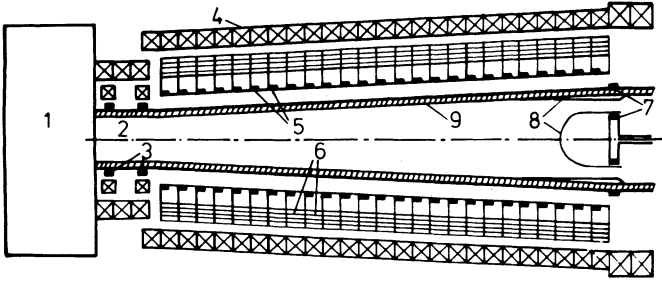


FIGURE 1 Schematic layout of SHERA.

directly after the separation or in the waiting-room as well. In the latter case, on the way back the ring is focused by its images in dielectric vacuum tube 9 with anisotropically conducting coating, which serves for shielding the rf radiation of the ring.

We consider below the following questions related to the scheme: requirements on the magnetic-field geometry, growth of ring emittance at the reflection, requirements on the pulse-line parameters, electron-ion ring stability and attainable output parameters of the accelerator.

### III. ACCELERATION AND SEPARATION OF THE RING COMPONENTS

1. Magnetostatic acceleration of electron-ion rings has been studied in Ref. 8. Proceeding from the generalized momentum conservation, adiabaticity of radial motion in a low-gradient magnetic field and conservation of total energy, the dependence of the ring major radius on  $B$  was found to be

$$r_0 = r_{0\text{in}} \sqrt{B_{z\text{in}}/B_z} \quad (2)$$

and the longitudinal relativistic factor is

$$\gamma_z = \frac{\xi_{\text{in}} + 1}{\xi_{\text{in}} + \sqrt{B_z/B_{z\text{in}}}} \quad (3)$$

Here  $\gamma_z = (1 - \beta_z^2)^{-1/2}$ ,  $v_z = c\beta_z$  is the axial velocity of the ring as a whole, and the subscript "in" marks the initial values.

In the case  $\xi_{\text{in}} \gg 1$ , the ring motion is essentially non-relativistic and

$$\beta_z^2 = \frac{2}{\xi_{\text{in}}} (1 - \sqrt{B_z/B_{z\text{in}}}) \quad (4)$$

While gaining the axial velocity, the ring expands both radially and axially, so that its holding power drops as  $r_0^{-2}(z)$ . Demanding the corresponding reduction in  $B_z = 0.5 r_0 \cdot \partial B_z / \partial z$  and making use of Eq. (2), we find the optimal magnetic-field profile

$$B_z(z) = \frac{B_{z\text{in}}}{(1 + \kappa z)^2} \quad (5)$$

The ring major radius is then a linear function of  $z$ . The constant  $\kappa$  is determined from

the holding condition (1) to be

$$\kappa = kf \frac{2v}{\beta_\theta^2 \gamma a_{in}} \quad (6)$$

where  $v = e^2 N_e / 2\pi r_0 m_e c^2$  is the Budker parameter  $a_{in} = (a_{rin} + a_{zin})/2$ .

From Eqs. (4) and (5), we find the acceleration length required to attain the preset final velocity  $c\beta_{zf}$  to be

$$l_{acc} = \frac{\xi_{in} \beta_{zf}^2}{2\kappa} \left( 1 - \frac{\xi_{in} \beta_{zf}^2}{2} \right)^{-1} \quad (7)$$

In the case  $N_i \rightarrow 0$ , the acceleration length<sup>7</sup> tends to a minimum value, proportional to the ratio of the final ion energy to the ring holding power. Assuming  $k = 0.25$  and the following values for the ring parameters:  $N_e = 10^{13}$ ,  $r_{0in} = 4$  cm,  $a_{in} = 2$  mm,  $Z/A = 0.08$ , we find from Eqs. (6) and (7) that the minimum length needed to gain an ion energy of 10 MeV per nucleon ( $\beta_{zf} \simeq 0.15$ ) is  $l_{acc} \simeq 8$  m. Letting the ring double its radius during acceleration, we get from Eqs. (2) and (4)  $\xi_{in} = \beta_{zf}^2 = 50$  and  $l_{acc} \simeq 15$  m. The corresponding number of uranium ions in a ring with  $\gamma_{in} = 25$  is  $N_i = 3 \cdot 10^{10}$ , so the neutralization factor is  $f = 0.06$ . This set of parameters will be used throughout and referred to as a "typical" set.

2. The problem of separation of accelerated ions from the electron ring without significant deterioration of the ring quality is a crucial one for the SHERA concept. An abrupt change in the strength of focusing while ions are shaken out excites oscillations of the minor dimensions of the ring and increases the ring emittance.<sup>5</sup>

If the betatron frequency is shifted instantly from  $\nu_1$  to  $\nu_2$ , then the growth of emittance, as defined by its rms characteristics, is given by the relations<sup>9</sup>

$$\frac{E_2}{E_1} = \frac{1}{2} \left( \frac{\nu_1}{\nu_2} + \frac{\nu_2}{\nu_1} \right), \quad (8)$$

which shows that the frequency shift should be as small as possible.

The external magnetic field provides effective radial focusing of electrons. The main problem is therefore to increase the axial electron frequency in the absence of ions. This problem can be solved by utilizing the focusing properties of the "squirrel cage" screen.<sup>7</sup> If the ratio of  $r_0$  to the screen radius  $r_{sc}$  is close to unity, then the post-separation betatron tunes are approximately

$$\nu_{z2}^2 \simeq \nu_w^2 \equiv \frac{2v}{\beta_\theta^2 \gamma g^2}, \quad \nu_{r2}^2 \simeq 1 - \nu_w^2, \quad (9)$$

where  $g = 2|r_{sc} - r_0|/r_0$ . The pre-separation electron tunes in a ring of annular cross-section are

$$\nu_1^2 = \nu_2^2 + Q_{ei}^2, Q_{ei}^2 \equiv f \frac{2v}{\beta_\theta^2 \gamma \alpha^2}, \quad (10)$$

with  $\alpha = a_0/r_0$  and  $a_0$  the minor ring radius. To focusing the spacing to the screen should be as small as the requirement  $2\nu_w^2 < 1$  coherent radial stability of the ring permits.

Under the real conditions, the emittance growth can differ from that Eq. (8) predicts. It is obvious that in order to minimize non-adiabaticity, the magnetic “hill” should not be too steep. On the other hand, when the gradient is low, the electrons trail behind the ions for a longer time, experiencing their defocusing (after separation) influence. Besides, the ions return a larger portion of energy back to the electrons, thus increasing the amplitude of the residual oscillations of the ring. Hence, there exists an optimum mirror-field configuration that makes the axial emittance growth a minimum.

The separation process has been simulated numerically making use of approximate equations obtained for fixed-ion ring dimensions and velocity:

$$\begin{aligned} \frac{d^2\xi_e}{d\tau^2} &= -Q_{ei}^2\alpha^2 \left[ \frac{\xi_e - \xi_i}{\alpha^2 + (\xi_e - \xi_i)^2} - \frac{\xi_e - \xi_i}{g^2 + (\xi_e - \xi_i)^2} \right] + \frac{B_r(\xi_e)}{B_0} \\ \frac{d^2\psi}{d\tau^2} &= - \left\{ v_w^2 - Q_{ei}^2\alpha^2 \frac{(\xi_e - \xi_i)^2 - \alpha^2}{[\alpha^2 + (\xi_e - \xi_i)^2]^2} - \frac{1}{B_0} \frac{\partial B_z}{\partial \xi_e} \right\} \psi + \frac{v_{z1}^2}{\psi^3}, \end{aligned} \quad (11)$$

where the dimensionless variables  $\xi = (z - z_{\min})/r_0$ ,  $\tau = v_\theta t/r_0$ ,  $\psi = a_z/a_0$  are introduced,  $z_{\min}$  is the axial position of the magnetic-field minimum, and  $B_0 = -m_e c^2 \beta_\theta \gamma / e r_0$ . The variation in the radial dimensions of the ring was also checked.

The optimum reflection conditions were sought in the special case of the mirror-field configuration

$$B_z = B_0(1 + n\xi^3/6 - n\xi x), \quad B_r = -B_0 n\xi^2/2, \quad (12)$$

where  $x = (r - r_0)/r_0$  and  $\xi > 0$ . The optimal values of field index  $n$  found at  $\beta_{zf} = 0.15$ , are well approximated by

$$n_{\text{opt}} \approx \frac{v_w^{5/2}}{3\sqrt{\alpha}}. \quad (13)$$

The growth of axial emittance at  $n = n_{\text{opt}}$  is determined by the ratio  $p = Q_{ei}^2/v_w^2 = fg^2/\alpha^2$  and depends weakly on other parameters. The numerical results presented in Fig. 2 show that irreversible growth of the rms axial size in a field of the considered geometry is 2 to 3 times less than in the case of instantaneous frequency shift (solid curve). A 1% increase in  $a_z$  occurs at  $p \approx 1$ , which at  $f = 0.06$  requires  $g \lesssim 4\alpha$ , i.e. the ring spacing to the screen should not exceed the ring minor diameter.

Although the magnetic field seen by the electrons varies little during reflection ( $\Delta B_z/B_z \simeq \beta_z^2/2 \sim 10^{-2}$ ), this variation is non-adiabatic and excites oscillations of the major ring radius with amplitude

$$\Delta r \sim \frac{2r_0}{\sqrt{1 - 2v_w^2}} \left( \frac{3\beta_z^5 f}{n} \right)^{1/3} \quad (14)$$

In a time of the inverse rotational frequency spread, the energy of coherent oscillations is transferred into incoherent motion, thus causing the radial half-width of the ring to grow by the magnitude<sup>9</sup>

$$\frac{\Delta a_2}{a_0} = \sqrt{1 + \left( \frac{\Delta z}{a_0} \right)^2} - 1. \quad (15)$$

With the typical ring parameters,  $n_{\text{opt}} \approx 0.2$  and Eq. (14) yields  $\Delta z \sim a_{of} = 4$  mm.

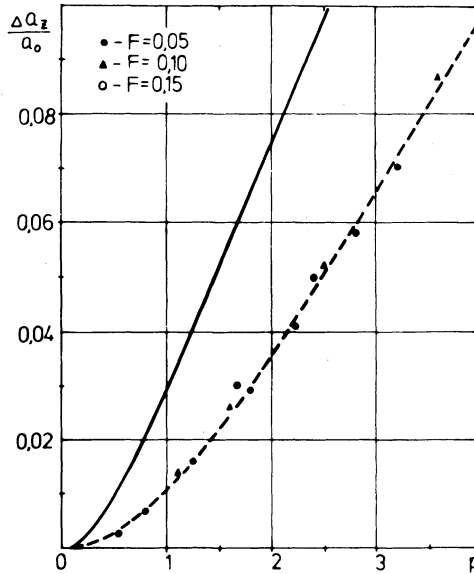


FIGURE 2 Irreversible growth of the axial rms dimension of the ring due to separation of ions. The solid curve corresponds to instantaneous frequency shift and the dashed curve to reflection by mirror field of optimal geometry.

Hence some additional coils or high-voltage electrodes are necessary to compensate for the variation in  $(B_z - \bar{B}_z/2)$ .

If the ring current is high, a passive electrically insulated coil or, in order to reduce  $\Delta B_z$ , a system of passive coils (see Fig. 1) can be applied to reflect the ring. By Lenz's law, the current induced in the coil by the oncoming ring retards the ring and in the case

$$\frac{2v}{\gamma} \sqrt{\frac{r_m}{r_0}} \left( \ln \frac{8\sqrt{r_0 r_m}}{|r_0 - r_m|} - 2 \right) \gtrsim \beta_{zf}^2, \quad (16)$$

where  $r_m$  is the coil radius, the retardation is sufficient for reflection. The essential advantage of passive coils is their high degree of magnetic-field axial symmetry due to the absence of connecting wires.

As computation shows, the electron ring axial energy increases insignificantly during separation (by 10 to 20%). Having shaken out the ions, the electron ring oscillates with amplitude  $\Delta z \approx I_{ace}/\xi_{in}$ . These oscillations are damped by Ohmic losses in the line and screens. Energy conversion into incoherent oscillations does not take place because the corresponding frequencies differ strongly.

#### IV. PULSE LINE

To return the electron ring to its initial state, a moving magnetic "piston" can be used, created by currents in coils of an artificial line.<sup>10</sup> The line represents a ladder network, one mesh of which is shown schematically in Fig. 3.

The basic parameters of the line must provide the required strength of radial component of the pulsed magnetic field ( $\bar{B}_2$ ) at the end of the line (EOL) where the

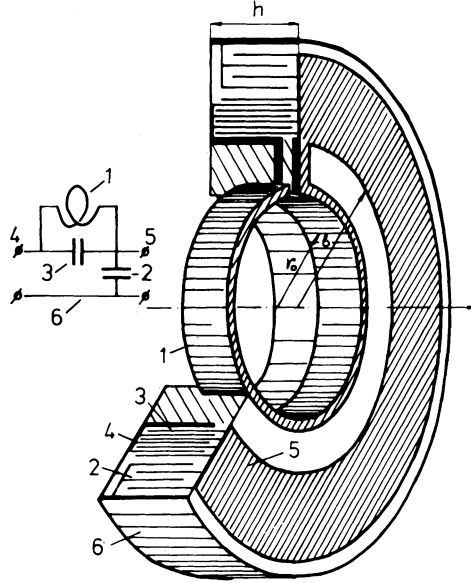


FIGURE 3 Equivalent scheme and preliminary design of the line element: 1—pulsed magnetic-field forming coil; 2—main capacitor  $C_0$ ; 3—Shunting capacitor  $C_1$ ; 4, 5,—surfaces of contact between adjacent elements; 6—return-current cylindrical conductor.

static field gradient is maximum. For this purpose, effective coupling of the ring to the line coils is needed, as well as a low level of Ohmic losses and phase distortions in the line.

In the case of harmonic time dependence of the line current,

$$\tilde{B}_r(z, t) = -\frac{I_0}{c} \frac{\partial}{\partial z} \operatorname{Re} \sum_{m=-\infty}^{\infty} \exp \left[ i \frac{\phi(z - v_\phi t) + 2\pi m z}{h} \right] g(l\phi + 2\pi m l), \quad (17)$$

where  $h$  is the line step and  $\phi$  is the phase shift between currents of amplitude  $I_0$  in adjacent coils. The coupling factor  $g$  is given by

$$g(\phi) = \frac{4\pi r_c}{h} I_1(\phi z_0/h) \left[ K_1(\phi r_c/h) - I_1(\phi r_c/h) \frac{K_1(\phi b/h)}{I_1(\phi b/h)} \right], \quad (18)$$

where  $r_c$  and  $b$  are the radii of the coils and inner conducting coating (see Fig. 3), and  $I_1(x)$  and  $K_1(x)$  are the modified Bessel and McDonald functions.

Measurements and calculations carried out in connection with the rapid-cycling compressor development revealed the essentially unfavorable influence of Ohmic losses and capacitors self-inductance on pulse propagation.<sup>11</sup> The design shown in Fig. 3 minimizes stray inductance and resistance of the line elements. The pulse distortion is caused mainly by phase-velocity dispersion due to inductive coupling between the line coils. The degree of distortion of a single pulse of duration  $\tau$  is characterized by the parameter

$$\eta = \kappa \left( \frac{4\phi_0}{\pi} \right)^3 \frac{l_{\text{acc}}}{h}, \quad (19)$$

where  $\phi_0$  is the phase shift corresponding to the main pulse frequency  $\omega_0 = \pi/\tau$ . The dispersion constant  $\kappa$  is determined by the line geometry and can be reduced by capacitive shunting of the coils:<sup>10</sup>

$$\kappa \approx \left(\frac{r_c}{2h}\right)^2 \left\{ 2 \cdot \left[ 1 - \left(\frac{r_c}{b}\right)^2 \right]^{-1} \cdot \ln \frac{b}{r_c} - 1 \right\} - \frac{C_1}{C_0}. \quad (20)$$

At  $\eta = 2$ , the decrease in the peak value of  $\tilde{B}_r$ , generated by a Gaussian current pulse is about 17%.

According to Eqs. (17) and (18), one must increase the phase shift  $\phi$  or to lessen the line step  $h$  in order to get higher  $\tilde{B}_r$  at fixed current amplitude. But then the distortion of the pulse would be enhanced, as Eq. (19) shows. The situation is made even more complicated by the retarding effect of the current induced in the line by the moving ring. In the steady state, the induced magnetic field seen by the ring is given by

$$B_r^{\text{ret}} = -\frac{2I_r r_0}{chL} \left(\frac{v_z}{v_{\phi 0}}\right)^2 \int_0^\pi \frac{\phi^4 \rho(\phi) g^2(\phi) d\phi}{4 \sin^2 \phi / 2 \cdot \{[(v_z/v_\phi(\phi))^2 - 1]^2 + \rho^2(\phi)\}}, \quad (21)$$

where  $I_r$  is the ring azimuthal current and  $\rho = \phi v_z R C_0 / (4h \sin^2 \phi / 2)$ ,  $R$  is the line element effective resistance<sup>10</sup> at frequency  $\omega = \phi v_z / h$  and

$$L \approx \frac{4\pi^2 r_c^2}{h} \left(1 - \frac{r_c^2}{b^2}\right) \quad (22)$$

is the element inductance with intercoil coupling and shielding effect of the coating included.<sup>10</sup> As follows from Eq. (21), increase of the  $g$ -factor and reduction of Ohmic losses and dispersion raise the retarding magnetic field.

Taking into account all pertinent requirements, determination of the optimum line parameters is a complicated problem and presently is not our objective. That it is possible to satisfy these requirements we shall illustrate with the following example. Let the *EOL* parameters be  $h = 4$  cm,  $r_c = 10$  cm,  $b = 14$  cm,  $C_0 = 0.14$   $\mu\text{F}$ . The phase velocity and the characteristic wave impedance correspondingly are  $v_{\phi 0}/c = h/\sqrt{LC_0} = 5 \cdot 10^{-4}$  and  $Z_w = 2$  Ohms. The dispersion of  $v_\phi$  at various values of  $C_1/C_0$  is shown in Fig. 4. In the absence of shunting ( $C_1 = 0$ ), the dispersion constant is  $\kappa = 0.55$ . The induced magnetic field dependence on the ring velocity found at  $r_0 = 4$  cm and  $I_r = 1.9$  kA is presented in Fig. 5. The plots show that  $B_r^{\text{ret}}$  can be greater by an order of magnitude than the radial component of static field  $B_r^{\text{st}}$ , equal to 30 G at the *EOL*.

The retarding effect may be significantly weakened if the requirement of strict synchronism between the ring and the pulse is given up, which is possible because of the finite interaction time. Permitting the ring to slip each pulse by a quarter pulse length ( $\pi h/4\phi_0$ ), we get a ring relative velocity  $v_z/v_\phi(\phi_0) = 1 - \pi h/4\phi_0 l_{\text{acc}} \approx 0.99$  at  $\phi_0 = 0.2$ . In Fig. 5, the points corresponding to this velocity are marked with circles. At  $C_1/C_0 = 0.22$ , we have  $B_r^{\text{ret}} = 15$  G.

Now we can find the peak current and voltage in the line. The pulsed field acting on the ring must be equal to  $|\tilde{B}_r| = B_r^{\text{st}} + B_r^{\text{ret}} = 45$  G at the *EOL*. Assuming this value to be 0.71 of the maximum, we obtain  $I_{of} = 3.5$  kA,  $U_{of} = 7$  kV in the case of a harmonic wave. The wave frequency is 120 kHz and the half-period  $\tau = 4$   $\mu\text{sec}$ . The maximum  $B_r$  value in a single pulse is approximately half that in a harmonic wave of the same current amplitude, so we have  $I_{of} \approx 7$  kA,  $U_{of} \approx 14$  kV.



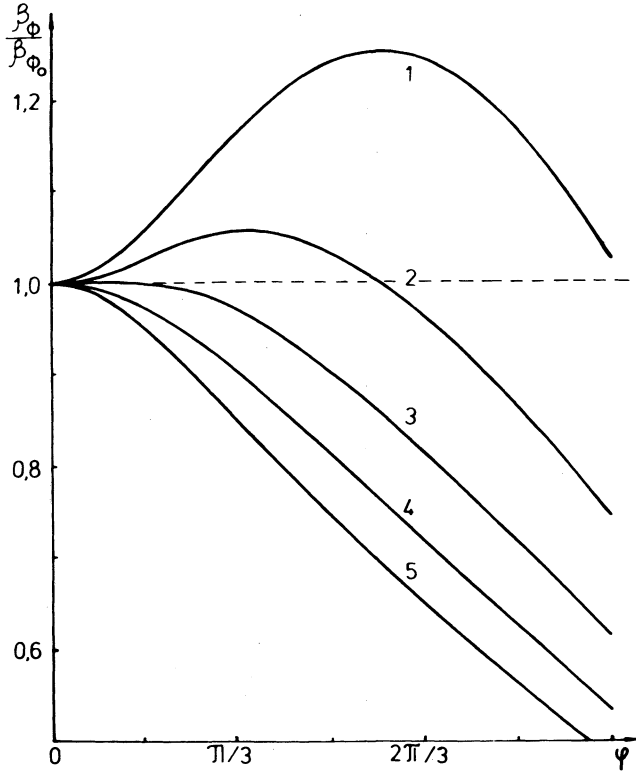


FIGURE 4 Relative phase velocity  $v_\phi(\phi)/v_{\phi 0}$  vs phase shift  $\phi$  for values of the ratio  $C_1/C_0$ : 1—0.0, 2—0.22, 3—0.44, 4—0.66, 5—0.88.

To determine the corresponding values at the line input, the decrease in  $\vec{B}$ , caused by Ohmic losses and dispersion, as well as by the variation in characteristic impedance, must be taken into account. Setting  $h = 4$  cm,  $r_c = 15$  cm,  $b = 19$  cm,  $C_0 = 0.09$   $\mu$ F ( $Z_w = 3$  Ohms) we get the peak values  $I_{oi} = 8$  kA,  $U_{oi} = 24$  kV, and the energy stored in the pulse  $W_{oi} = 0.5$  kJ.

Though not optimum, the figures obtained are typical for pulsed systems of accelerators; their attainability is assured.

## V. ELECTRON-ION RING STABILITY

A number of instabilities leading to deterioration of ring quality have been observed in experiments on formation and acceleration of electron-ion rings.<sup>2,3,12</sup> The most restrictive constraints on the compressed ring parameters are imposed by the negative-mass instability<sup>2,3</sup> (self-bunching) and the electron-ion dipole instability.<sup>2,12</sup> There is also some danger in crossing the integer resonance of electron radial oscillations<sup>2</sup> at the start, which gives rise to a radial shift of the ring as a whole.

1. The negative-mass instability can be suppressed by conducting structures close to the ring.<sup>2</sup> The requirement of low energy losses of the pulse magnetic field precludes the use of solid screens. Hence it seems reasonable to apply an anisotropically conducting screen formed by two coaxial cylinders slit along the axis so that the strips of one

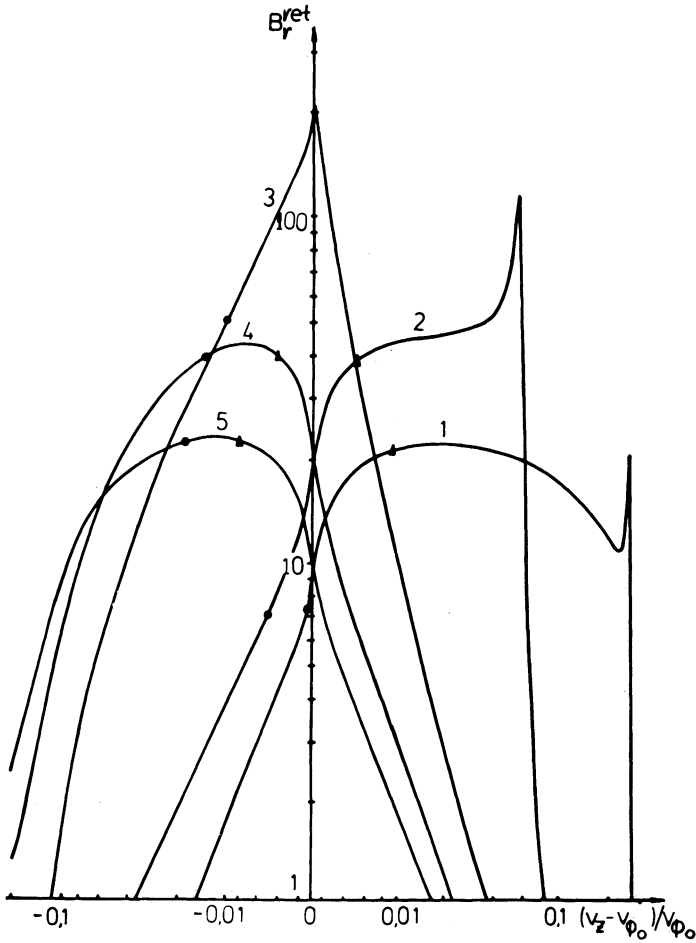


FIGURE 5 Dependence of the retarding magnetic field  $B_r^{\text{ret}}$  on the relative ring velocity  $(v_z/v_{\phi_0} - 1)$  for the same values as in Fig. 4 values of  $C_1/C_0$ .

- ▲ —  $v_z = v_{\phi_0}(\phi_0), \phi_0 = 0.2$
- —  $v_z = 0.99 \cdot v_{\phi_0}(\phi_0)$

cylinder capacitively bridge the slits of the other.<sup>13</sup> This configuration may be called “a double squirrel cage”, in contrast to the ordinary squirrel cages placed in the separation region. The screen cross-section is shown schematically in Fig. 6.

The wavelength is large compared with the strip width  $H$  and the screen properties are therefore characterized by the parameter

$$\alpha = \frac{2\Delta N}{\pi H} \approx \frac{\Delta N^2}{\pi^2 r_{sc}^2}, \tag{23}$$

where  $N$  is the number of strips in each cylinder,  $r_{sc}$  is the inner screen radius, and  $\Delta$  and  $\epsilon$  are the width and dielectric constant of the insulating layer.

The effect of shielding on the ring stability against self-bunching is usually treated in terms of coupling impedance.<sup>2,14</sup> The coupling impedance of an ordinary squirrel cage

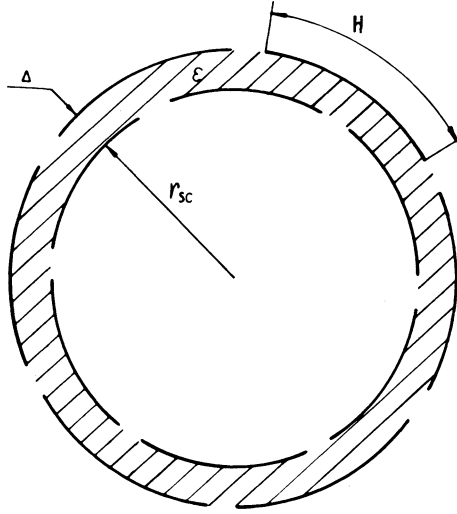


FIGURE 6 Cross section of modified squirrel cage.

is found to exceed significantly the impedance of the ring in free space as a consequence of excitation of a *TEM* wave propagating along the slits.<sup>15</sup> The contribution of *TEM* modes to the impedance may be regarded as a measure of the shielding of the ring rf field. In the case of the double screen with  $2\alpha \lesssim \sqrt{\epsilon - 1}$ , the *TEM* impedance is approximately<sup>13</sup>

$$Z_n^{TEM} = Z_0 \frac{\pi\alpha r_0}{\sqrt{\epsilon} r_{sc}} \exp \left[ -2n\sqrt{\epsilon - 1} \left( \frac{r_{sc}}{r_0} - 1 \right) \right], \quad (24)$$

where  $n$  is the azimuthal harmonic number of the excited field, and  $Z_0 = 4\pi/c$  (120 $\pi$  Ohms in practical units).

The level of shielding of the pulsed magnetic field is given in turn by the coefficient<sup>13</sup>

$$f_0 = \frac{x^2 I_1(x) K_1(x)}{x^2 I_1(x) K_1(x) + \alpha}, \quad (25)$$

where  $x = |k_z| r_{sc}$  and  $k_z = \phi_0/h$  is the propagation constant at the main pulse frequency. It is easier to keep both the impedance and  $f_0$  small at high  $\epsilon$ : the induced rf current is loaded on the squirrel cage by overlapping parts of the strip transmission lines with characteristic impedance proportional to  $\epsilon^{-1/2}$ , whereas for quasi-stationary azimuthal current the slits are equivalent to inductances which are independent of  $\epsilon$ .

Let us take for example  $r_0/r_{sc} = 0.7$  (so that the ring does not excite TE modes with azimuthal numbers  $n = 1, 2$ ) and  $\epsilon = 5$ . Then to provide  $Z_1^{TEM} \leq 60$  Ohms,  $\alpha \leq 0.9$  is needed. With the pulse line parameters chosen in the previous section we have  $x = 0.14 \div 0.28$  and Eq. (25) the drop in  $\vec{B}_r$  does not exceed 8%. In the beginning of the acceleration section, the value  $\alpha = 0.9$  may be obtained with  $\Delta = 0.4$  mm and  $N = 36$  ( $h = 1$  cm).

2. The electron-ion dipole instability has a resonant character and occurs at definite frequencies of oscillations of the ring components.<sup>16</sup> The boundaries of the instability

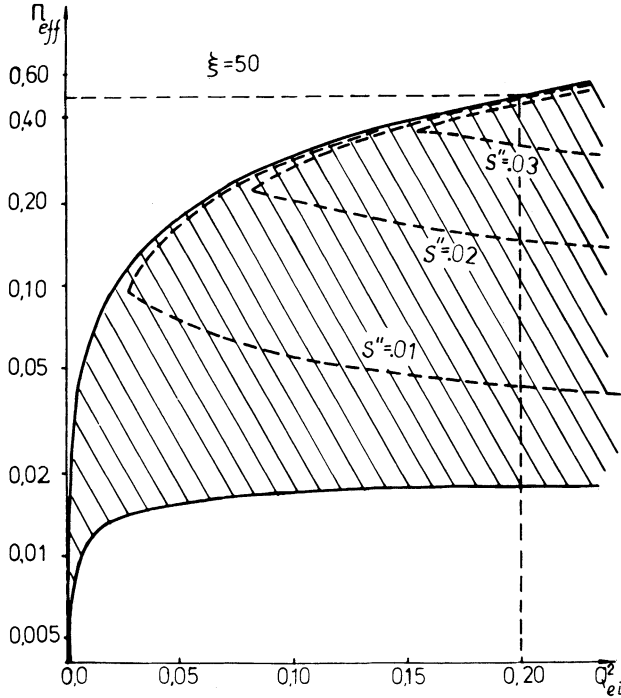


FIGURE 7 Electron-ion dipole instability domain in  $Q_{ei}^2, n_{eff}$ -plane at  $\xi = 50$ . Curves of equal growth rate  $S'' = \text{Im } \omega / \omega_H$ , where  $\omega_H$  is the electron gyrofrequency, are shown with dashes.

region in the  $Q_{ei}^2, n_{eff}$ -plane found at  $\xi = 50$  with neglect of incoherent frequency spread and nonlinearity in self-fields, are shown in Fig. 7. Here  $n_{eff} = n + 2v_w^2$  for radial and  $n_{eff} = 1 - n$  for axial instability, where  $n$  is the conventional external magnetic-field index, and  $\xi, Q_{ei}^2$  and  $v_w$  are defined in Section III.

As Fig. 7 shows, the ring with "typical" parameters ( $Q_{ei}^2 = 0.2$ ) requires for stability either  $n_{eff} \geq 0.5$  or  $n_{eff} \leq 0.018$ . Therefore the field index in the "waiting-room" must be close to  $n = 0.5$ . The spacing between the ring and dielectric tube (or modified squirrel cage) in the acceleration section should be chosen so that  $v_w^2 \leq 0.01$ . Let us notice that nonlinear Landau damping, which was neglected here, must reduce the instability domain.

3. When the ring is pushed into the acceleration section or when it enters the separation region, the electron coherent radial frequency  $Q_r = \sqrt{1 - n_{eff}}$  changes abruptly; although image focusing prevents the crossing of the  $Q_r = 1$  resonance, the proximity of  $Q_r$  in the acceleration section to the resonant value may cause a large shift of the ring as a whole with respect to the accelerator axis<sup>2</sup>

$$\Delta r = \frac{r_0}{n_{eff}} \cdot \frac{\delta B_z}{B_z}, \quad (26)$$

where  $\delta B_z$  is the amplitude of the azimuthal modulation of static field. In the region of separation,  $n_{eff}$  is much higher because of the additional squirrel cages ( $n_{eff} \approx 0.4$ ). When the ring enters this region, the non-adiabatic change in  $n_{eff}$  excites a ring

precession with amplitude equal to its initial off-centering from Eq. (26), and eventually makes the radial width of the ring grow in accordance with Eq. (15).

Requiring  $\Delta r/a_0 \leq 0.15$ , which corresponds to a 1% width growth, and assuming  $n_{\text{eff}} = 0.02$ ,  $a_0/r_0 = 0.05$ , from Eq. (26) we get a tolerance for the first-harmonic amplitude  $\delta B_z/B_z < 1.5 \cdot 10^{-4}$  which is common in accelerator technology. The tolerance for alignment of the additional screens to the solenoid axis follows from the same limitation  $\Delta r/a_0 \leq 0.15$  and at  $a_0 = 4$  mm is  $\Delta r \leq 0.5$  mm.

## VI. SHERA OUTPUT PARAMETERS

In the quantitative analysis, we have used the following set of the ring parameters:  $N_e = 10^{13}$ ,  $r_{\text{in}} = 4$  cm,  $a_{\text{in}} = 2$  mm,  $\gamma_{\text{in}} = 25$ . The number of uranium ions in a ring  $N_i = 3 \cdot 10^{10}$  corresponds to a loading factor  $\xi_{\text{in}} = 50$ ; at  $Z/A = 0.08$  the neutralization factor is  $f = 0.06$ . To gain an ion energy of 10 MeV/nucleon, an acceleration length  $l_{\text{acc}} = 15$  m is necessary. The ring doubles its dimensions at this length.

The output ion current depends on the total number of cycles of acceleration by each electron ring and on the repetition rate. The exposure time necessary to reach the ion charge state  $Z = 19$  by electron impact ionization does not exceed 1 msec, so a ring cycling frequency of 1 kHz is possible. The lifetime of each electron ring is limited mainly by three factors: synchrotron-radiation loss, electron multiple scattering by the stored ions and the non-adiabatic separation process. Let us consider these effects separately.

The electron energy loss by radiation does not exceed 10% in 20 msec time. To keep  $\xi_{\text{in}}$  and consequently the ion final energy constant, the number of ions  $N_i$  should be reduced correspondingly from cycle to cycle. This does not break the holding condition of Eq. (1) because the ring dimensions are damped as  $\gamma$  by synchrotron radiation. Due to the decrease in major radius, the ring spacing from the squirrel cage grows in the separation region. To compensate for the corresponding fall in image focusing, a second screen interior to the ring should be added as shown in Fig. 1.

In the case of a ring with annular cross-section, the enlargement of its minor radius caused by multiple scattering is approximately

$$\frac{\Delta a}{a_0} = \left[ 1 + t \frac{8e^4 r_0 N_i Z_A^2}{\pi m_e^2 C^3 v_0^2 a_0^4 \gamma^2} \ln(1g2\gamma Z_A^{-1/3}) \right]^{1/4} - 1, \quad (27)$$

where  $Z_A$  denotes the atomic number of stored ions, and  $v_0 = v_r = v_z$  is the electron betatron tune. With a field index in the waiting-room  $n = 0.5$  and  $Q_{et}^2 = 0.2$ , we have  $v_r^2 = v_z^2 = 0.7$  and Eq. (27) yields  $\Delta a/a_0 \approx 20\%$  in the  $t = 20$  msec scattering time.

Approximately the same increase in minor dimensions ( $\approx 16\%$ ) is caused by 20 reflections of the ring by the magnetic mirror. But the resultant total enlargement is about 30%, for each of these factors significantly weakens the effect of the other. This enlargement is quite admissible and corresponds to the upper limit of the safety factor  $k = 0.33$ .

Thus 20 msec may be accepted as the ring life time, which permits the ring to be used 20 times. Assuming 50 pps as a repetition rate of the electron ring generator, we have a total of  $10^3$  cycles of acceleration per second and a corresponding uranium beam intensity of  $3 \cdot 10^{13}$  ions per second.

For estimates we have taken figures that are neither optimal nor extreme. Increasing the number of electrons  $N_e$  and the ring dimensions as  $N_e^{1/3}$ , which leaves the stability requirements intact, it is possible to magnify the output ion current. At an achievable figure,  $N_e = 3 \cdot 10^{13}$ , we have a uranium-beam intensity of nearly  $10^{14}$  ips, and in the case of light ions, because of the shorter time needed for their stripping, an intensity of up to  $10^{16}$  ips.

## VII. ACKNOWLEDGMENTS

We would like to express our gratitude to Drs. N. Yu. Kazarinov, A. B. Kuznetsov, E. A. Perelstein and B. G. Schinov for stimulating discussions.

## REFERENCES

1. V. I. Veksler et al., *Proc. IV Internat. Conf. on High Energy Accelerators*, Cambridge, USA, p. 289 (1967).
2. V. P. Sarantsev and E. A. Perelstein, *Collective Acceleration of Ions by Electron Rings* (Atomizdat., Moscow, 1979).
3. A. Faltens et al., *Proc. IX Internat. Conf. on High Energy Accelerators*, Stanford, USA, p. 226 (1974).
4. M. L. Iovnovich et al., Joint Institute for Nuclear Research Report JINR P9-11686, Dubna (1978).
5. I. M. Kapchinsky, Institute for Theoretical and Experimental Physics Report ITEF-63, Moscow (1973).
6. L. S. Barabash et al., JINR Report P9-11776, Dubna (1978).
7. G. V. Dolbilov et al., JINR Report P9-4737, Dubna (1969).
8. W. B. Lewis, in *Symposium on ERA, LRL*, Berkeley, California, p. 195 (1968).
9. N. Yu. Kazarinov et al., *Particle Accelerators*, **10**, 33 (1980).
10. Yu. I. Alexahin, JINR Report P9-82-843, Dubna (1982).
11. V. S. Aleksandrov et al., JINR Report P9-80-625, Dubna (1980).
12. C. Andelfinger et al., *Proc. IX Intern. Conf. on High Energy Accelerators*, Stanford, USA, p. 218 (1974).
13. Yu. I. Alexahin, JINR Report P9-83-813, Dubna (1983).
14. Yu. I. Alexahin and J. Habanec, *Czech. Journ. of Physics*, **B31**, 544 (1981).
15. P. Merkel, Max-Planck Institut für Plasmaphysik IPP 0/39, Garching (1979).
16. B. V. Chirikov, *Atomnaya Energiya*, **19**, 239 (1965).
17. J. D. Jackson, *Classical Electrodynamics* (Wiley and Sons, Inc., New York, 1975), 2nd ed., pp 648–649.